Macromolecules

Article

pubs.acs.org/Macromolecules

Solution Behavior of Double-Hydrophilic Block Copolymers in Dilute Aqueous Solution

Olivier Casse,[†] Andriy Shkilnyy,[‡,§,%] Jürgen Linders,[∥] Christian Mayer,[∥] Daniel Häussinger,[†] Antje Völkel,[‡] Andreas F. Thünemann,[⊥] Rumiana Dimova,[#] Helmut Cölfen,[‡,&] Wolfgang Meier,[†] Helmut Schlaad,*[,‡] and Andreas Taubert*[,‡,§]

[†]Department of Chemistry, University of Basel, Klingelbergstrasse 80, CH-4056 Basel, Switzerland

[‡]Department of Colloid Chemistry, Max Planck Institute of Colloids and Interfaces, Research Campus Golm, D-14424 Potsdam, Germany

[§]Institute of Chemistry, University of Potsdam, Karl-Liebknecht-Straße 24-25, D-14476 Golm, Germany

[∥]Institute of Physical Chemistry, University of Duisburg-Essen, CeNIDE, Universitätsstraße 2, D-45141 Essen, Germany

[⊥]BAM Federal Institute for Materials Research and Testing, Unter den Eichen 87, D-12205 Berlin, Germany

[#]Department of Theory and Biosystems, Max Planck Institute of Colloids and Interfaces, Research Campus Golm, D-14424 Potsdam, Germany

[&]Physical Chemistry, University of Konstanz, Universitätsstraße 10, D-78457 Konstanz, Germany

ABSTRACT: The self-assembly of double-hydrophilic poly(ethylene oxide)−poly(2-methyl-2-oxazoline) diblock copolymers in water has been studied. Isothermal titration calorimetry, small-angle X-ray scattering, and analytical ultracentrifugation suggest that only single polymer chains are present in solution. In contrast, light scattering and transmission electron microscopy detect aggregates with radii of ca. 100 nm. Pulsed field gradient NMR spectroscopy confirms the presence of aggregates, although only 2% of the polymer chains undergo aggregation. Water uptake experiments indicate differences in the hydrophilicity of the two blocks, which is believed to be the origin of the unexpected aggregation behavior (in accordance with an earlier study by Ke et al. [*Macromolecules* **2009**, *42*, 5339−5344]). The data therefore suggest that even in double-hydrophilic block copolymers, differences in hydrophilicity are sufficient to drive polymer aggregation, a phenomenon that has largely been overlooked or ignored so far.

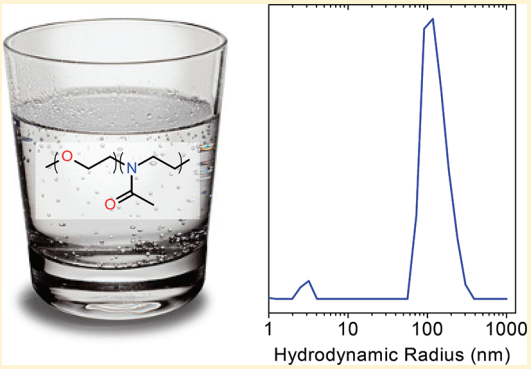

INTRODUCTION

Self-assembling molecular systems have attracted a tremendous interest over the past years. Because of the potential biological applications, low molecular weight compounds like lipids[1,2] but also macromolecules have been widely studied in aqueous solutions.[3−5] A particular class of water-soluble macromolecules, double-hydrophilic diblock copolymers (DHBCs, polymers with only hydrophilic but no hydrophobic blocks), has attracted great attention.[6,7] DHBCs have been intensely studied as stimuli-responsive materials[8−11] and for their role in mineralization control of inorganic compounds.[6,12,13]

Although DHBCs are an intriguing class of materials, virtually no data on the behavior of pure DHBCs in aqueous solution exist. It is assumed in the literature that, unless triggered with an appropriate chemical (pH, ionic strength, complexation), physical (temperature, electric and magnetic field) or biochemical (enzymes, ligands) stimulus, these copolymers exist in dilute solution as single molecules in a random coil conformation.[14]

In spite of this, a few reports state that some DHBCs aggregate in pure water. Several independent studies have described the aggregation of poly(ethylene oxide)-*block*-poly(*N*-isopropylacrylamide) (PEO-*b*-PNIPAM) and poly(*N*-isopropylacrylamide)-*graft*-poly(ethylene oxide) (PNIPAM-*g*-PEO) copolymers even below the lower critical solution temperature (LCST) of PNIPAM in water.[15−21] Attempts to explain this behavior include the suggestion by Berlinova et al.[15,19] that, as PNIPAM is quite hydrophobic at ambient temperature, it forms hydrophobic domains stabilized by the more hydrophilic PEO blocks affording micelle-like structures. A similar behavior was reported by Huang et al.[22] in poly(ethylene glycol)-*block*-poly[*trans*-*N*-(2-ethoxy-1,3-dioxan-5-yl)acrylamide] (PEG-*b*-PtNEA) block copolymer solutions. Below its LCST, the polymer shows a bimodal distribution in

Received: March 29, 2012
Revised: May 9, 2012
Published: May 22, 2012

   dx.doi.org/10.1021/ma300621g | *Macromolecules* 2012, 45, 4772−4777

dynamic light scattering (DLS) indicating some association. The PtNEA block was held responsible for the association because the PtNEA homopolymer also associates below its LCST in water. From the evaluation of the scattered intensity in light scattering the authors concluded that the weight fraction of the assemblies is very small compared to the single chains.

Some non-stimulus-responsive polymers also form aggregates, the most prominent study being published by Ke et al.[14] The authors focused on loose aggregates formed in water by a poly(ethylene glycol)-*block*-poly(*N*,*N*-dimethylacrylamide) (PEG-*b*-PDMA) block copolymer. The aggregates show a weak concentration and temperature dependence as well as an opposite salt effect and are in equilibrium with the respective unimers. Investigation of these aggregates in different conditions (additives, etc.) led to the conclusion that the driving force for polymer association is the incompatibility between the two blocks, mainly caused by their different capacity to interact with water.

In concentrated solution, poly(ethylene oxide)-*block*-poly(2-methyl-2-oxazoline) (PEO-*b*-PMOXA) copolymers form unique water-in-water (W/W) mesophases, in both the absence and presence of salt.[23] Above polymer weight fractions of ca. 0.5 in water, sticky and birefringent solids form. Using polarization microscopy, a lamellar and a hexagonal lyotropic mesophase have tentatively been assigned, although no detailed analysis of the mesophase could be carried out. This was mainly due to the lack of contrast in small-angle X-ray scattering. A more recent study by Armes and co-workers, however, found a series of well-defined body-centered cubic, hexagonal, or lamellar lyotropic phases in concentrated aqueous solutions of poly(ethylene oxide)-*block*-poly[2-(methacryloyloxy)-ethylphosphorylcholine) (PEO-*b*-PMPC) diblock copolymers. Among others, the authors reported the occurrence of double-hydrated lamellar phases, where both polymer blocks are hydrated, but to a different extent.[24]

The current study is an extension of our earlier work[23] into the dilute regime, showing that PEO−PMOXA block copolymers coexist as single chains and aggregates in water. Large aggregates, as detected by light scattering and electron microscopy, are formed by just 2% or less of the chains, quantified by diffusion NMR experiments.

EXPERIMENTAL PART

Polymer Synthesis and Characterization. All chemicals and PEO (number-average molecular weight, M_n = 4.7 kg/mol, 107 repeat units) were purchased from Sigma-Aldrich. PMOXA (M_n = 10.5 kg/mol, 118 repeat units) was synthesized by ring-opening polymerization of 2-methyl-2-oxazoline (MOXA) initiated by methyl tosylate (MeOTos) in acetonitrile. PEO−PMOXA block copolymer samples were prepared as previously reported:[23,25,26] PEO monomethyl ether was tosylated, to yield PEO-OTos, in dry toluene under argon in the presence of an excess of tri(m)ethylamine. The ammonium chloride was filtered off, and the polymer was precipitated into petrol ether. The crude product was twice dissolved in chloroform and precipitated into diethyl ether and finally freeze-dried from benzene. The PEO-OTos was then used to initiate the ring-opening polymerization of MOXA in acetonitrile. The polymerization was carried out at reflux temperature (~80 °C) for 20 h. After cooling to room temperature, the acetonitrile was removed via rotary evaporation. The polymers were twice dissolved in chloroform and precipitated into petrol ether and finally freeze-dried from benzene; molecular characteristics of the PEO−PMOXA samples are summarized in Table 1. ^{1}H NMR ($CDCl_3$ 300 MHz, ppm): 1.98−2.22 (CH_3CON), 3.48 (NCH_2CH_2), 3.64 (OCH_2CH_2). IR (KBr, cm^{-1}): 3441 (m, H_2O), 2885 (m, CH), 1637 (s, CNR), 1426 (m, CH), 1359 (w, CH), 1243 (w, CN), 1148 (w, CO), 1104 (s, CC). Elemental analysis: PEO_{107}−$PMOXA_{64}$, C 53.88%; N 3,73%; H 10.53%; PEO_{107}−$PMOXA_{112}$, C 53.62%; N 10.31%; H 10.43%.

Table 1. Molecular Characteristics of the Polymers Used in the Current Study

sample	x_{PMOXA}[a]	M_n (kg/mol)[b]	$(M_w/M_n)^{app}$[c]	M_w^{app} (kg/mol)[d]
PEO_{107}		4.7		
$PMOXA_{118}$		10.5		
PEO_{107}−$PMOXA_{64}$	0.38	10.1	1.87	18.9
PEO_{107}−$PMOXA_{112}$	0.51	14.2	1.56	22.2

[a]Mole fraction of PMOXA (^{1}H NMR). [b]Number-average molecular weight (^{1}H NMR). [c]Polydispersity index (SEC; DMSO + 5 mg/mL LiBr, 70 °C, calibration: pullulan). [d]Weight-average molecular weight, $M_w^{app} = M_n(M_w/M_n)^{app}$.

Isothermal Titration Calorimetry. ITC measurements were performed with a VP-ITC microcalorimeter (MicroCal Inc., Northampton, MA). All solutions were degassed shortly before the measurements. The working cell (WC, 1.442 mL in volume) and the reference cell were filled with water. The injection syringe was loaded with PEO_{107}−$PMOXA_{64}$ solution of different concentrations. Each experiment consisted of a series of injections of 5 or 10 μL of the polymer solution into the WC. During measurement, the solution was constantly stirred at 310 rpm at 25 °C. The differential power needed to compensate the released heat to maintain zero temperature difference between sample and reference cells after the injection of the polymer solution was recorded vs time. Integration of the individual calorimetry traces yields the heat released at each injection step. Data analysis was carried out with Origin (MicroCal).

Small-Angle X-ray Scattering (SAXS). SAXS measurements were performed at the BAMline at the Synchrotron BESSY II (Berlin, Germany) with a Kratky-type instrument (SAXSess from Anton Paar, Austria) at 25 ± 1 °C. The SAXSess has a low sample-to-detector distance (0.309 m), which is appropriate for investigation of dispersions with low scattering intensities. The measured intensity was corrected by subtracting the intensity of a capillary filled with pure solvent. The scattering vector is defined in terms of the scattering angle θ and the wavelength λ of the radiation (λ = 0.124 nm): thus, $q = 4\pi/\lambda \sin\theta$. Deconvolution (slit length desmearing) of the SAXS curves was performed with Glatter's established indirect Fourier transformation method implemented in the PCG Software Version 2.02.05 (University of Graz).[27−29]

Analytical Ultracentrifugation. AUC was performed on a Beckman-Coulter XL-I ultracentrifuge with UV/vis-absorption and Rayleigh interference optics. Experiments were carried out at 25 °C in self-made titanium double-sector centerpieces using interference detection. Sedimentation−velocity experiments were performed with 5−40 mg/mL polymer solutions at 60 000 rpm. Sedimentation coefficient distributions $g^*(s)$ were evaluated without diffusion correction using the program SEDFIT.[30] Sedimentation−equilibrium experiments were performed with 0.1−5 mg/mL polymer solutions at 30 000−45 000 rpm. Molar masses were evaluated using the program MSTAR.[31] The partial specific volume of the polymer (PEO_{107}−$PMOXA_{64}$: $\bar{\nu}$ = 0.809 mL/g) was determined with a DMA 5000 density oscillation tube (Anton Paar, Graz, Austria).

Light Scattering. Solutions for light scattering were prepared from a stock solution of 60 mg/mL. Dilutions to 10 mg/mL were measured, but below 20 mg/mL, the scattering intensity was too low for analysis. Samples were filtered through Millipore filters (0.45 μm, Millex-HV) into 10 mm quartz cells mounted in an optical matching bath. Static (SLS) and dynamic light scattering (DLS) experiments were done with a commercial goniometer (ALV) with a He:Ne laser (JDS Uniphase, λ = 632.8 nm). Scattering angles were between 30° and 150°, and the photon intensity autocorrelation function $g_2(t)$ was

dx.doi.org/10.1021/ma300621g | Macromolecules 2012, 45, 4772−4777

determined with an ALV-5000E correlator. The experiments were performed at $T = 20 \pm 0.02$ °C. The refractive index increment dn/dc = 0.1600 mL/g (PEO_{107}–$PMOXA_{112}$) and 0.1516 (PEO_{107}–$PMOXA_{64}$) was measured with an ALV-DR1 differential refractometer (λ = 632.8 nm) at 20 °C. Data were analyzed via the Zimm plot, and nonlinear decay-time analysis was supported by a regularized CONTIN algorithm.

Electron Microscopy. Polymers were dissolved in water under mild overnight stirring. 3–5 μL of the solution were deposited on carbon/parlodion-coated TEM copper grids and allowed to dry at room temperature. Samples were stained for 30 s with 6% uranyl acetate, and images were taken on an FEI Morgani 268D with a tungsten filament operated at 80 kV.

Diffusion NMR. After addition of 72 mg glucose per 1 mL of polymer solution as a diffusion tracer, the samples were transferred to conventional 5 mm NMR tubes. Diffusion NMR spectra were obtained on an Avance 400 spectrometer (Bruker, Karlsruhe) with a field gradient unit on proton signals at 400 MHz. A stimulated echo sequence combined with two field gradient pulses was applied, resulting in an echo signal of an intensity which generally depends on the average displacement of the observed molecules as well as the settings of the pulse strength G, the pulse duration δ, and the spacing Δ between the two pulses. The pulse strength G was varied between 0 and 680 G/cm, the duration of the pulse δ was 1.0 ms, and the pulse spacing Δ was 50, 100, or 200 ms. The echo signals were Fourier transformed to the corresponding frequency spectra showing the different dependencies of the signal intensities on G and Δ. The signals at 3.497 and 3.126 ppm were used as characteristic signal positions for the polymer and for the diffusion tracer, glucose, respectively.

Water Uptake Experiments. Water uptake experiments were carried out in a desiccator at constant humidity (84%) over saturated potassium nitrate solution at 18 and 25 °C. Samples were removed from the desiccator for gravimetric analyses.

RESULTS

Isothermal titration calorimetry (ITC) of the polymer solutions (concentration range up to 13.5 mg/mL) only detects a signal assigned to heat of dilution (data not shown), suggesting that the polymers are dissolved in water as single chains. Small-angle X-ray scattering (SAXS) supports this observation as only scattering curves from individual chains are observed. The shape of the SAXS scattering curves is constant within a concentration range of 0.5–4.0 wt %, and the simplest model for a sufficient interpretation of the SAXS data is the random coil model. An example for a curve fit is shown in Figure 1 for PEO_{107}–$PMOXA_{64}$. The pattern of the scattering intensity is horizontal toward the lowest attainable q-value of 0.07 nm^{-1}.

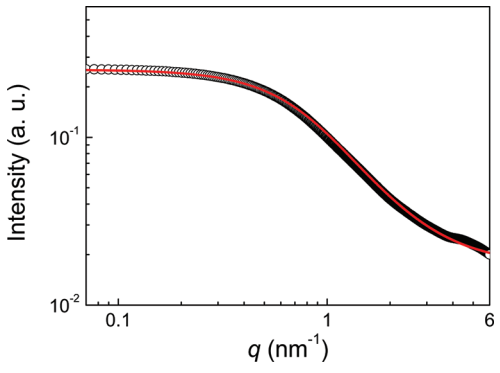

Figure 1. SAXS pattern of PEO_{107}–$PMOXA_{64}$ at 2 wt % in water (symbols) and a curve fit (line) using the Gaussian chain model with a radius of gyration of 2.0 ± 0.1 nm. T = 25 °C.

Therefore, no aggregates with sizes up to the SAXS detection limit of $\pi/0.07$ nm^{-1} = 45 nm are visible.

Figure 2 shows the sedimentation coefficient distributions, $g^*(s)$, obtained from analytical ultracentrifugation (AUC) of

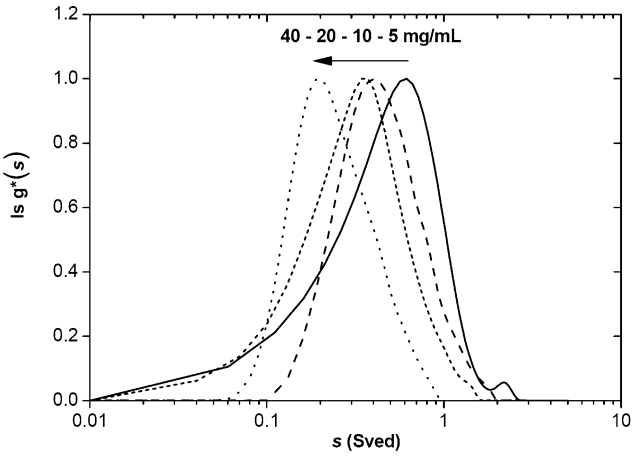

Figure 2. AUC sedimentation coefficient distributions $g^*(s)$ of PEO_{107}–$PMOXA_{64}$ at 0.5–4 wt % in water. T = 25 °C.

aqueous solutions of PEO_{107}–$PMOXA_{64}$ at concentrations of 0.5–4 wt %. All distributions are rather broad, as expected for synthetic polymers; it may also be an effect of diffusion broadening. Moreover, the maximum shifts from s_{max} = 0.6 Sv (0.5 wt %) to 0.2 Sv (4 wt %). These results suggest that, indeed, there are no aggregates in solution, and the polymers are molecularly dissolved. The fact that AUC does not detect any aggregates may be due to the low refractive index increment, suggesting a high amount of water in the aggregates. The shift in s_{max} is assigned to some nonideality from polymer–polymer interaction, changes in viscosity, and crowding.[32] Sedimentation–equilibrium data for PEO_{107}–$PMOXA_{64}$ support this, as polymer concentrations of 0.01–0.5 wt % yield weight-average molecular weights of 15.9 kg/mol, which is in reasonable agreement with the M_w obtained from NMR/SEC for single chains (M_w^{app} = 18.9 kg/mol, Table 1).

In spite of the above results, light scattering (Figure 3) shows that there is some polymer aggregation. For PEO_{107}–$PMOXA_{64}$ in water, dynamic light scattering (DLS) and nonlinear lag-time analysis[33] by double-exponential fitting of the autocorrelation function reveals two distinct populations of decay times, which differ by 2 orders of magnitude. Converted to hydrodynamic radii (R_h), these two populations have sizes that are characteristic for single polymer chains, R_h = 2.4 ± 1.4 nm, and for aggregates, R_h = 104 ± 25 nm. Data for PEO_{107}–$PMOXA_{112}$ have been inconclusive as it behaves more "gel-like". There, the Zimm plot could not be analyzed, and DLS shows a larger apparent R_h of 270 ± 18 and 4.0 ± 0.3 nm for aggregates and single chains, respectively.

Static light scattering (SLS) supports DLS and finds a radius of gyration R_g of 103 ± 5 nm for PEO_{107}–$PMOXA_{64}$ using the hard-sphere model.[33−36] The second virial coefficient is essentially zero within the experimental error (A_2 = (−0.5 ± 3) × 10^{-6} mol cm^3/g^2), and the apparent weight-average molar mass of the aggregates is M_w^{app} = 257 ± 5 kg/mol. It must be noted that NMR spectroscopy (see below) indicates that the true concentration of the polymer chains in the aggregates is much lower than the nominal polymer concentration, only 1.8 mol % at c_0 = 2 wt % (20 mg/mL). As a result, SLS

dx.doi.org/10.1021/ma300621g | Macromolecules 2012, 45, 4772–4777

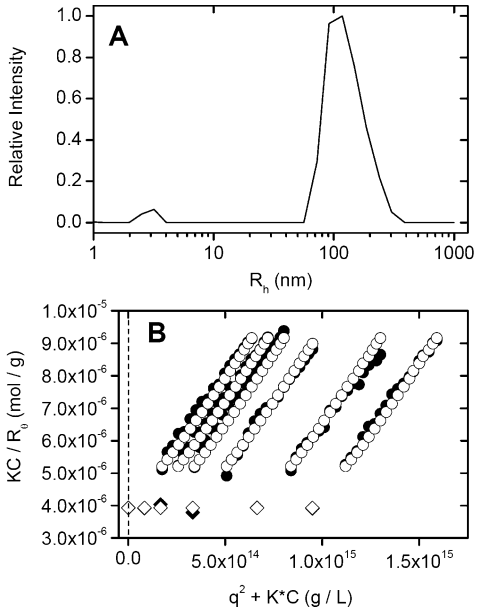

Figure 3. Light scattering data from PEO_{107}–$PMOXA_{64}$ in aqueous solution: (A) Contin plot from DLS, (B) Zimm plot from SLS. Solid symbols in (B) are experimental data, open symbols are simulations of scattering of a hard sphere. Diamonds are q^2 extrapolated to 0 (experimental and simulated, respectively). T = 20 °C.

underestimates the molar mass of the aggregates. Re-evaluation of the SLS data accounting for the low fraction of aggregates yields M_w^{app} = 14 300 ± 300 kg/mol and an aggregation number of $Z = M_w^{app}/M_w^{polymer} \sim 750$. The aggregation number Z is too low for a vesicle of that size, although the ratio $\rho = R_g/R_h \approx 1$ unity would suggest the presence of a vesicular structure with a thin membrane.[33] This therefore implies that, although light scattering suggests vesicular structures, the aggregates may in fact not be vesicles but some other highly hydrated species. Spherical micelles can definitely be excluded because R_h is larger than the contour length (all-trans conformation, 107 × 0.36 nm + 64 × 0.36 nm ≈ 60 nm) of the polymer.

Transmission electron microscopy (TEM) confirms the presence of spherical aggregates. Figure 4 shows a representative TEM image of collapsed aggregates of PEO_{107}–$PMOXA_{64}$ at 2 wt % in water. The aggregates are roughly spherical with a radius of 25–75 nm. This is consistent with light scattering if some shrinking due to the high vacuum conditions and the high water content in the aggregates is taken into account. TEM also shows that the aggregates are probably not very stable, as the

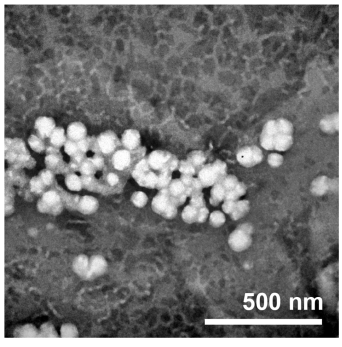

Figure 4. TEM image of collapsed aggregates of PEO_{107}–$PMOXA_{64}$ at 2 wt % in water.

negatively stained samples also show features in the background, mostly thin lines. These lines could be smaller polymer aggregates, but a clear assignment is currently not possible.

It is obvious that a comparison between an aqueous polymer solution and a dried collapsed sample on a TEM grid is not straightforward. Attempts to image the aggregates by cryogenic TEM failed (data not shown), probably due to insufficient contrast between continuous phase and hydrated aggregates. Nevertheless, TEM qualitatively supports light scattering results and shows that the double-hydrophilic block copolymer PEO–PMOXA self-assembles into relatively well-defined, but probably unstable, spherical aggregates at polymer concentrations above 1 wt %.

To reconcile the DLS/SLS and TEM data (suggesting the presence of aggregates) with the corresponding AUC, SAXS, and ITC results (neither of which detect aggregates; this is likely due to the low aggregate concentration and/or poor contrast and sensitivity), diffusion NMR spectroscopy was employed. In these experiments, tracer molecules encapsulated by (or associated with) polymer aggregates are separated from the external fraction (in bulk solution) by their diffusion behavior yielding a different signal decay than freely diffusing low molecular species.[37−40] For detection of a possible encapsulated volume phase, glucose was added to the polymer solutions as an additional tracer for the pulsed field gradient (PFG) NMR measurements (Figure 5). In the given case, PFG-

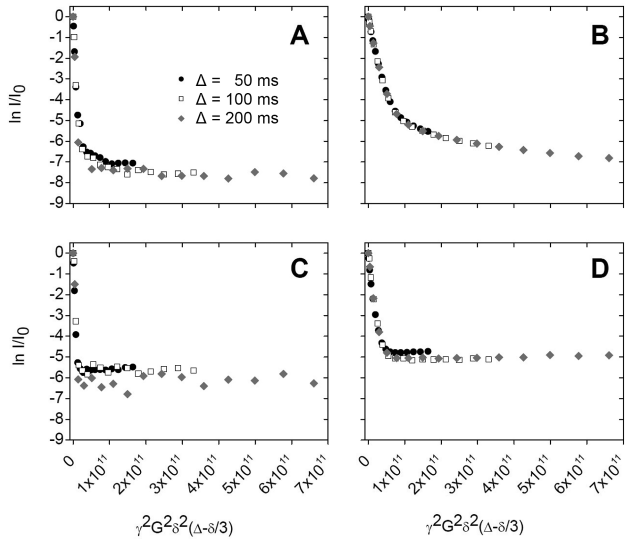

Figure 5. PFG-NMR data from glucose and polymer solutions. Relative echo signal intensities are plotted logarithmically vs a function of the gradient strength G and the pulse spacing Δ. (A) Self-diffusion pattern of glucose in a solution of aggregates of PEO_{107}–$PMOXA_{64}$, (B) self-diffusion pattern of individual PEO_{107}–$PMOXA_{64}$ molecules in a solution of aggregates, (C) self-diffusion pattern of glucose in a solution of aggregates of PEO_{107}–$PMOXA_{112}$, and (D) self-diffusion pattern of individual PEO_{107}–$PMOXA_{112}$ molecules in a solution of aggregates. T = 25 °C.

NMR is based on the combination of a stimulated echo sequence with two field gradient pulses. The gradient strength G as well as the spacing Δ between the gradient pulses of duration δ is systematically varied, leading to a set of echo decay patterns revealing the self-diffusion behavior of any molecule labeled with a nucleus with a given gyromagnetic ratio γ. For free diffusion, a logarithmic plot of the relative echo

dx.doi.org/10.1021/ma300621g | Macromolecules 2012, 45, 4772–4777

intensity I/I_0 vs the parameter $\gamma^2G^2\delta^2(\Delta - \delta/3)$ gives a straight line with a slope equal to the negative self-diffusion coefficient.

The first part of the analysis focuses on the glucose tracer identified via a signal at 3.126 ppm. Figure 5A,C clearly shows that two different fractions of glucose molecules are present in both solutions: the freely diffusing molecules in the bulk solution (corresponding to the initial steep decay) and a smaller fraction with limited self-diffusion, representing the portion of tracer molecules encapsulated inside the polymer aggregates (indicated by the flat part of the plot). Free diffusion is observed for the majority of the glucose molecules down to a value of $\ln(I/I_0) = -6$ for PEO_{107}–$PMOXA_{64}$ and −5.5 for PEO_{107}–$PMOXA_{112}$.

The volume fraction of the encapsulated glucose fractions can be estimated from an extrapolation of the flat parts of the plots in Figure 5A,C. The intersections with the ordinate axis near $\ln(I/I_0) \approx -6$ and −5.5 imply that the approximate relative contributions of the encapsulated fractions amount to $I/I_0 \approx \exp(-6) \approx 0.0025$ for PEO_{107}–$PMOXA_{64}$ and to $I/I_0 \approx \exp(-5.5) \approx 0.004$ for PEO_{107}–$PMOXA_{112}$. Hence, the flat sections of the plots represent 0.25 or 0.4 mol %, respectively, of the overall glucose which undergoes limited self-diffusion. The slopes for the encapsulated species level off at very small values which cannot be quantified but which are compatible with the Brownian motion of spheres with radii near 100 nm.[41]

The PFG-NMR experiments also allow for an estimation of the permeability of the aggregates. When the spacing Δ between the two gradient pulses is increased and comes into the same range as the exchange rate between the free and the associated state of the glucose molecules, the echo signals for the encapsulated species exhibits a characteristic decrease.[37−40] The corresponding data show no significant dependence on Δ in a range between 50 and 200 ms. This suggests that the molecular exchange of glucose between associated and free species is negligible within this time span.

An analogous analysis can be performed on the echo intensities for a hydrogen position of the polymer itself (methylene groups of the PEO residue represented by a signal at 3.497 ppm). This allows for a quantification of the fraction of the polymer which takes part in the formation of aggregates at a given point in time and for the exchange rate between the free and associated state. In the case of PEO_{107}–$PMOXA_{64}$ it is difficult to separate the mobile from the immobile fraction because there is no clear transition between the two parts of the plot (Figure 5B). In a rough estimation, one may localize the intersection of the shallow part near $I/I_0 \approx \exp(-4) \approx 0.018$. This implies that 1.8% of the polymer contribute to aggregates while 98.2% are single chains. In the case of PEO_{107}–$PMOXA_{112}$, the separation is much clearer (Figure 5D). An intersection at $I/I_0 \approx \exp(-5) \approx 0.0067$ indicates that 0.67% of the overall polymer contribute to aggregates. In both cases, the exchange between the free and the associated state is relatively slow: no significant loss in the echo intensity is detected within 200 ms.

DISCUSSION

We have studied the behavior of two water-soluble PEO–PMOXA block copolymers in aqueous solution. While ITC, SAXS (Figure 1), and AUC (Figure 2) suggest that the polymers are dissolved on a molecular level, DLS/SLS (Figure 3) and TEM (Figure 4) show the presence of aggregates in aqueous solution. PFG-NMR (Figure 5) reveals an equilibrium between single chains and aggregates where the aggregate fraction is below 2%. The results therefore support an earlier study by Huang et al.[22] on PEG-*b*-PtNEA block copolymer solutions, where also aggregates were observed as well. Similar to the current data, the aggregate concentration was very low.

The components of the polymers under investigation here, PEO and PMOXA, are water-soluble, but they are chemically different. A key question therefore is whether or not one block is significantly more hydrophilic than the other one, similar to a previous study[14] suggesting that the two blocks have a significantly different capability for interaction with water. This could lead to a strongly preferred water uptake by one of the blocks, leading to a water gradient in the resulting aggregates and thus incompatible blocks. In order to evaluate hydrophilicity differences between the blocks, we subjected PEO and PMOXA homopolymers to water uptake experiments under controlled atmosphere, the results of which are shown in Figure 6. Indeed, PMOXA takes up roughly 10 times more

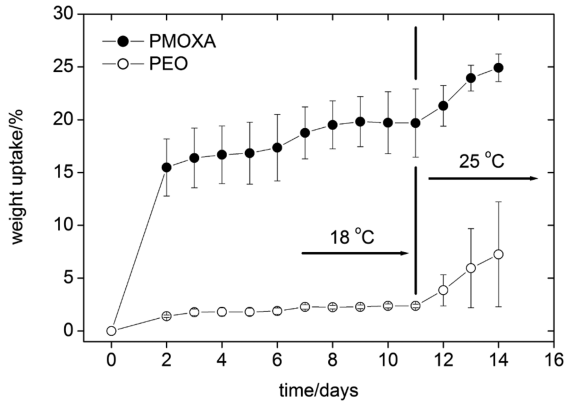

Figure 6. Water uptake of PEO_{107} and $PMOXA_{118}$ homopolymers.

water (by weight) than PEO at 18 °C. Both polymers show an increased water uptake at 25 °C, but still PEO is much less prone to water uptake. Presumably, the roughly identical uptake at 25 °C is due to the fact that the polymers are already saturated to some extent.

From the ITC data suggesting that the polymers are present as single chains and the water uptake data, the number of water molecules per monomer unit can be estimated, assuming that each monomer unit in the PEO chain needs three water molecules for complete solubilization.[42] A simple calculation based on the molecular weight, the number of repeat units of each block, and the water/monomer unit ratio shows that, accordingly, each PMOXA monomer unit needs ca. 5.2 water molecules for complete solubilization. Taking into account the concentration of water molecules, which is ∼55.5 mol/L, the molar ratio of water molecules to monomer units is roughly 100 in our experiments. This number far exceeds the required excess of ca. 5-fold, and we therefore presume that each monomer unit is fully hydrated.

Overall, the current study shows that in PEO–PMOXA copolymers with two hydrophilic blocks there is indeed one block, PMOXA, that can take up much more water than the other one, PEO. This is consistent (on a macroscopic level) with the hypothesis described above.[14] The previous and the current data therefore suggest that polymer aggregates cannot form by entropy gain, as is the case for amphiphilic block copolymers. Because the polymers are hydrophilic, they probably do not release water (at least not a significant amount

dx.doi.org/10.1021/ma300621g | *Macromolecules* 2012, 45, 4772–4777

and not even the PEO block), and therefore the entropic contribution to aggregation is likely minimal. Since PMOXA binds more water molecules than PEO, we (and Ke et al.[14] and Blanazs et al.[24]) postulate the presence of two "phases" containing different amounts of water molecules. Such an arrangement can be viewed as "graded hydrophilicity". The assembly of such a construct would then be governed by the Laplace pressure (due to interfacial energy, $\Pi_i = 2\gamma/R$, where γ is the interfacial tension; this is not to be confused with the γ utilized in the NMR experiments, Figure 5) and osmotic pressure (due to a different number of water molecules per unit volume). Aggregates would be stable once the difference between pressures is zero. Possibly this determines the sizes of the aggregates, but more information will be needed to further confirm or deny this hypothesis. On a different note, such a behavior could also be responsible for the formation of W/W mesophases;[23,24] once in their different hydration state, the blocks may phase separate similar to a polymer swollen in a weakly selective solvent.

CONCLUSION

The current article clearly shows that nonionic double-hydrophilic block copolymers also aggregate in dilute aqueous solution. They form highly swollen and rather well-defined spherical aggregates. PFG-NMR shows that the fraction of aggregates is below 2%. Water uptake experiments suggest that a hypothesis put forward by Ke et al.[14] claiming that the fraction of water taken up by each block is a ruling parameter governing self-assembly is correct. This implies, and the current data confirm this, that there is another effect besides the hydrophobic effect and amphiphilic interactions, which we term graded hydrophilicity, to account for the fact that differences in hydrophilicity appear to be sufficient to drive aqueous self-assembly. This makes the controlled self-assembly of double-hydrophilic block copolymers all the more fascinating and potentially useful.

AUTHOR INFORMATION

Corresponding Author

*E-mail schlaad@mpikg.mpg.de, Ph ++49 (0)331 567 9514 (H.S.); e-mail ataubert@uni-potsdam.de, Ph ++49 (0)331 977 5773 (A.T.).

Present Address

[%]Department of Chemical and Biotechnological Engineering, Université de Sherbrooke, QC J1H 5N4, Canada.

Notes

The authors declare no competing financial interest.

ACKNOWLEDGMENTS

We thank Dr. T. Sottmann (Univ. Köln) for neutron scattering measurements (not included in this work). We thank the EU-RTN "POLYAMPHI", BIOSONS, the Swiss National Science Foundation, the Swiss Nanoscience Institute, and the Max Planck Society for financial support. A.T. thanks the Holcim Stiftung Wissen for a (long expired) habilitation fellowship. A.S. acknowledges a Max Planck postdoctoral fellowship.

REFERENCES

(1) Tanford, C. *Science* **1978**, *200*, 1012.
(2) Whitesides, G. M.; Mathias, J. P.; Seto, C. T. *Science* **1991**, *254*, 1312.
(3) Cui, H.; Chen, Z.; Zhong, S.; Wooley, K. L.; Pochan, D. J. *Science* **2007**, *317*, 647.
(4) Discher, D. E.; Eisenberg, A. *Science* **2002**, *297*, 967.
(5) Förster, S.; Plantenberg, T. *Angew. Chem., Int. Ed.* **2002**, *41*, 688.
(6) Cölfen, H. *Macromol. Rapid Commun.* **2001**, *22*, 219.
(7) Ge, Z. S.; Liu, S. Y. *Macromol. Rapid Commun.* **2009**, *30*, 1523.
(8) de las Heras Alarcon, C.; Pennadam, S.; Alexander, C. *Chem. Soc. Rev.* **2005**, *34*, 276.
(9) Lazzari, M.; Liu, G.; Lecommandoux, S. *Block Copolymers in Nanoscience*; Wiley: New York, 2006.
(10) Rodríguez-Hernández, J.; Chécot, F.; Gnanou, Y.; Lecommandoux, S. *Prog. Polym. Sci.* **2005**, *30*, 691.
(11) Schmaljohann, D. *Adv. Drug Delivery Rev.* **2006**, *58*, 1655.
(12) Cölfen, H.; Mann, S. *Angew. Chem., Int. Ed.* **2003**, *42*, 2350.
(13) Cölfen, H.; Qi, L. *Chem.—Eur. J.* **2001**, *7*, 106.
(14) Ke, F.; Mo, X.; Yang, R.; Wang, Y.; Liang, D. *Macromolecules* **2009**, *42*, 5339.
(15) Berlinova, I.; Iliev, N.; Vladimirov, P.; Novakov, C. *J. Polym. Sci., Part A: Polym. Chem.* **2007**, *45*, 4720.
(16) Kjøniksen, A.-L.; Nyström, B.; Tenhu, H. *Colloids Surf., A* **2003**, *228*, 75.
(17) Kjøniksen, A.-L.; Zhu, K.; Pamies, R.; Nyström, B. *J. Phys. Chem. B* **2008**, *112*, 3294.
(18) Motokawa, R.; Morishita, K.; Koizumi, S.; Nakahira, T.; Annaka, M. *Macromolecules* **2005**, *38*, 5748.
(19) Nedelcheva, A., N.; Vladimirov, N., G.; Novakov, C., P.; Berlinova, I., V. *J. Polym. Sci., Part A: Polym. Chem.* **2004**, *42*, 5736.
(20) Topp, M. D. C.; Dijkstra, P. J.; Talsma, H.; Feijen, J. *Macromolecules* **1997**, *30*, 8518.
(21) Zhao, J.; Zhang, G.; Pispas, S. *J. Polym. Sci., Part A: Polym. Chem.* **2009**, *47*, 4099.
(22) Huang, X.; Du, F.; Cheng, J.; Dong, Y.; Liang, D.; Ji, S.; Lin, S.-S.; Li, Z. *Macromolecules* **2009**, *42*, 783.
(23) Taubert, A.; Furrer, E.; Meier, W. *Chem. Commun.* **2004**, 2170.
(24) Blanazs, A.; Warren, N. J.; Lewis, A. L.; Armes, S. P.; Ryan, A. J. *Soft Matter* **2011**, *7*, 6399.
(25) Kind, L.; Shkilnyy, A.; Schlaad, H.; Meier, W.; Taubert, A. *Colloid Polym. Sci.* **2010**, *288*, 1645.
(26) Stoenescu, R.; Meier, W. *Mol. Cryst. Liq. Cryst.* **2004**, *417*, 185.
(27) Glatter, O. *J. Appl. Crystallogr.* **1977**, *10*, 415.
(28) Glatter, O.; Kratky, O. *Small-Angle X-Ray Scattering*; Academic Press: London, 1982.
(29) Fritz, G.; Glatter, O. *J. Phys.: Condens. Matter* **2006**, *18*, S2403.
(30) Schuck, P. *Biophys. J.* **2000**, *78*, 1606.
(31) Cölfen, H.; Harding, S. E. *Eur. Biophys. J. Biophys. Lett.* **1997**, *25*, 333.
(32) Yphantis, D. A.; Roark, D. E. *Biochemistry* **1971**, *10*, 3241.
(33) Burchard, P.; Patterson, G. D. *Light Scattering from Polymers*; Springer: Berlin, 1983; Vol. *48*.
(34) Wyatt, P. J. *Anal. Chim. Acta* **1993**, *272*, 1.
(35) Zimm, B. H. *J. Chem. Phys.* **1948**, *16*, 1093.
(36) Zimm, B. H. *J. Chem. Phys.* **1948**, *16*, 1099.
(37) Bauer, A.; Hauschild, S.; Stolzenburg, M.; Förster, S.; Mayer, C. *Chem. Phys. Lett.* **2006**, *419*, 430.
(38) Leson, A.; Filiz, V.; Förster, S.; Mayer, C. *Chem. Phys. Lett.* **2007**, *444*, 268.
(39) Rumplecker, A.; Forster, S.; Zahres, M.; Mayer, C. *J. Chem. Phys.* **2004**, *120*, 8740.
(40) Yan, Y.; Hoffmann, H.; Leson, A.; Mayer, C. *J. Phys. Chem. B* **2007**, *111*, 6161.
(41) Smoluchowski, M. *Ann. Phys.* **1906**, *21*, 756.
(42) Smart, T. P.; Mykhaylyk, O. O.; Ryan, A. J.; Battaglia, G. *Soft Matter* **2009**, *5*, 3607.

NOTE ADDED AFTER ASAP PUBLICATION

This paper was published on the Web on May 22, 2012. Figure 5, the Acknowledgments, and ref 8 have been revised. The correct version was reposted on May 24, 2012.